

# Temperature dependent $d-d$ excitations in manganites probed by resonant inelastic x-ray scattering

S. Grenier,<sup>1,2</sup> J. P. Hill,<sup>2</sup> V. Kiryukhin,<sup>1</sup> W. Ku,<sup>2</sup> Y.-J. Kim,<sup>2</sup> K. J. Thomas,<sup>2</sup> S.-W. Cheong,<sup>1</sup> Y. Tokura,<sup>3</sup> Y. Tomioka,<sup>3</sup> D. Casa,<sup>4</sup> and T. Gog<sup>4</sup>

<sup>1</sup>*Department of Physics and Astronomy, Rutgers University, Piscataway, New Jersey 08854, USA*

<sup>2</sup>*Department of Physics, Brookhaven National Laboratory, Upton, New York 11973, USA*

<sup>3</sup>*Joint Research Center for Atom Technology (JRCAT), Tsukuba 305-0046, Japan*

<sup>4</sup>*CMC-CAT, Advanced Photon Source, Argonne National Laboratory, Argonne, Illinois 60439, USA*

(Dated: July 25, 2018)

We report the observation of temperature dependent electronic excitations in various manganites utilizing resonant inelastic x-ray scattering (RIXS) at the Mn  $K$ -edge. Excitations were observed between 1.5 and 16 eV with temperature dependence found as high as 10 eV. The change in spectral weight between 1.5 and 5 eV was found to be related to the magnetic order and independent of the conductivity. On the basis of LDA+ $U$  and Wannier function calculations, this dependence is associated with intersite  $d-d$  excitations. Finally, the connection between the RIXS cross-section and the loss function is addressed.

PACS numbers: 75.47.Lx, 61.10.-i, 74.25.Jb, 71.27.+a

Manganites of the form  $\text{RE}_{1-x}\text{AE}_x\text{MnO}_3$  where RE is a trivalent rare earth and AE a divalent alkali earth, exhibit a diverse range of magnetic and electronic phases. The recent theoretical and experimental studies have focussed on identifying the electronic ground states and the potential role of phase inhomogeneities [1, 2]. However, details of the origin and nature of the electronic order remain elusive. What is known is that the various phases are stabilized through cooperative and competing interactions involving the spin, orbital, charge and electron-lattice degrees of freedom of the states derived from the Mn  $3d$  and the O  $2p$  bands.

Current models frequently integrate out the oxygen degrees of freedom and parameterize the behavior of the Mn  $3d$  orbitals with terms such as the hopping amplitude between neighboring Mn sites, the on-site Coulomb repulsion ( $U$ ) and the Hund's coupling ( $J_H$ ), each of which are on the order of several eV. Experimental measurements of the excitation spectra up to these energies can thus play a key role in the understanding of these systems - in particular such measurements provide far more stringent tests of the various theoretical approaches than do ground state measurements. Central to such efforts will be understanding how the excitation spectrum relates to the various magnetic and electronic orderings.

In this paper, we report resonant inelastic x-ray scattering studies of the electronic excitation spectrum in a number of manganites, for a range of ground states. We find that in all samples, the excitation spectra show systematic temperature dependencies associated with the magnetic ordering at energy scales up to 10 eV. The integrated spectral weight in the 1 eV to 5 eV energy range increases on entering ferromagnetic phases, decreases for antiferromagnetic spin alignment, and is unchanged through metal-insulator transitions for which the magnetic ground state is unchanged. On the basis of time-dependent density functional calculations, we argue that this temperature dependence arises from intersite  $d-d$  excitations which are suppressed or enhanced for antiferromagnetic or ferromagnetic nearest-neighbor spin correlations, respectively. These results both point to the sensitivity of RIXS to

magnetic order and to the need for realistic calculations of the  $q$ -dependent dielectric function.

Inelastic x-ray scattering (IXS), like optical measurements, is a photon in - photon out probe of electronic excitations over energy scales up to and above the charge-transfer gap. Both techniques have recently been applied to the manganites [3, 4, 5, 6]. IXS offers the additional advantage that one can measure dispersion of the excitations over the entire  $q$ -space with bulk sensitivity. Further, by tuning the photon energy to the absorption edge (or "resonance") the IXS cross-section may be enhanced, allowing even high- $Z$  based systems to be studied [7, 8] - albeit at the price of a more complicated cross-section. Recently, Resonant IXS (RIXS) has been utilized to study  $\text{LaMnO}_3$  [6] where it was argued that the technique revealed excitations related to the ordering of orbitals.

In the present work, samples with several magnetic, orbital, charge and structural ground states were studied:  $\text{La}_{0.875}\text{Sr}_{0.125}\text{MnO}_3$  (hereafter referred as LSMO.125) which has a paramagnetic semi-conductor (PMSC) to ferromagnetic metal (FM) phase transition at 190 K and is a ferromagnetic insulator (FI) below 150 K;  $\text{La}_{0.7}\text{Ca}_{0.3}\text{MnO}_3$  (LCMO.3) which is PMSC above  $T_C = 250$  K and FM below;  $\text{Pr}_{0.6}\text{Ca}_{0.4}\text{MnO}_3$  (PCMO.4) which undergoes a phase transition from PMSC to a two-dimensional antiferromagnetic insulator (AFI) at 234 K with the onset of orbital ordering, and becomes a three-dimensional antiferromagnetic insulator (AFI) at  $T_N = 180$  K; and  $\text{Nd}_{0.5}\text{Sr}_{0.5}\text{MnO}_3$  (NSMO.5) which has a PMSC to FM transition at 250 K, and a FM to orbitally ordered AFI transition at 150 K. All samples were grown by the floating zone method. Their quality was checked by x-ray diffraction, resistivity measurements and magnetization measurements using a commercial SQUID.

The experiments were performed at beamline 9IDB, CMC-CAT at the Advanced Photon Source. Successive Si(111) and Si(311) monochromators were used. The scattered x-rays were collected by a spherically bent Ge(531) analyzer and focused onto a solid-state detector. The overall resolution was 300 meV (FWHM). The incident photons were linearly po-

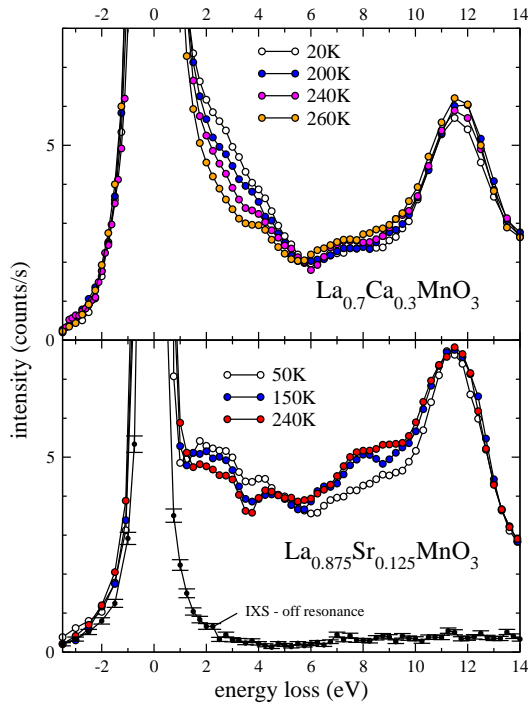


FIG. 1: Energy loss spectra of LSMO.125 and LCMO.3 vs temperature. Each point is averaged over three consecutive data points to decrease the statistical noise. The elastic line (0 eV) was typically 3000 counts/s for LCMO.3 and 1000 counts/s for LSMO.125, error bars are typically .15 counts/s. An off-resonance spectrum is shown in the lower panel ( $E_i=6538$  eV).

larized, perpendicular to the scattering plane. The incident energy,  $E_i$ , was tuned to the peak of the Mn  $K$ -edge absorption of the respective materials - for which the RIXS intensity was maximized (this varied from  $E_i = 6555$  to  $6557$  eV with increasing doping). The data were taken at  $Q=(0\ 2.3\ 0)$ ,  $Pbnm$  settings, which minimized the number of elastically scattered photons. Typical inelastic count rates were between 1 and 10 counts/s. The background, as measured on the energy gain side, was  $\sim 0.1$  count/s. The  $K_{\beta 5}$  emission line, i.e. decays from the Mn  $3d$  band, occurs at  $6534$  eV, i.e. out of the range of the present scans which cover the energy  $E_i + 3$  to  $E_i - 14$  eV. Here, the inelastic scattering arises following the recombination of the exciton comprised of the  $1s$  core-hole and the  $4p$  photo-electron, after it has exchanged energy with the valence electrons.

Inelastic spectra for LCMO.3 and LSMO.125 are shown in Fig. 1. In each case, data were taken on cooling from a paramagnetic semiconducting phase into a ferromagnetic phase: Temperature dependence is apparent up to 10 eV. The spectra are characterized by three distinct regions: The region up to 6 eV energy loss, which shows an increase in spectral weight on cooling into the respective ferromagnetic phases, a region between 6 and 10 eV which shows little or opposite temperature dependence; and a peak at around 12 eV with no systematic temperature dependence. In what follows, we will focus primarily on the region below 6 eV.

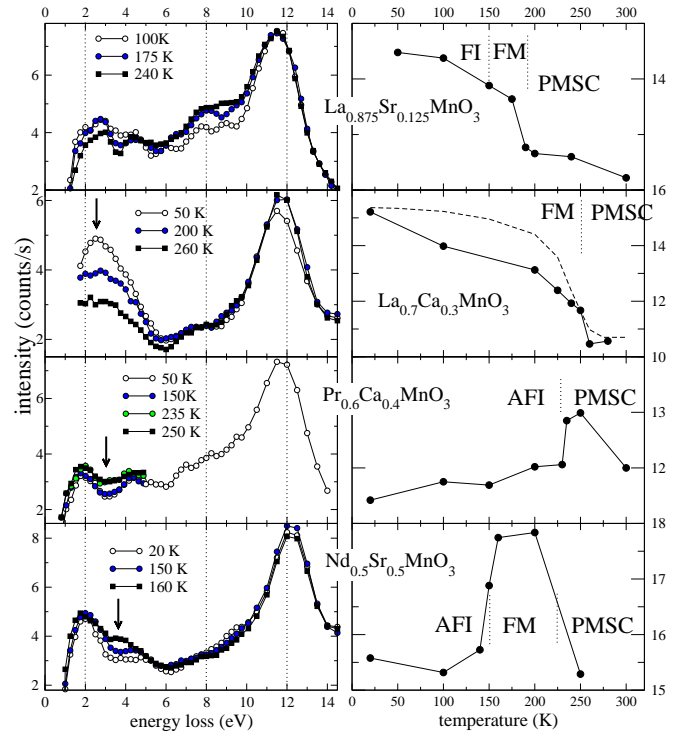


FIG. 2: (Left) Selected energy loss spectra vs temperature after subtraction of the quasi-elastic line. The arrow indicates the region of maximum temperature dependence. (Right) Integrated spectral intensity between 1.5 and 5 eV. For LCMO.3, the increase is shown to relate to the magnetization (dashed line, taken from ref. [9])

To do so quantitatively, we must first subtract the elastic scattering, which increases with temperature as a result of quasi-elastic scattering from phonons. This was carried out by assuming that the elastic line is symmetric and subtracting the energy-gain side from the energy-loss side. This assumption was shown to be valid by measuring the elastic scattering off-resonance (Fig. 1). We believe this procedure gives reliable spectra above 1.5 eV. The results for the four samples are shown in the left panels of Fig. 2.

In all samples, the lowest energy feature in the subtracted spectra occurs at  $\sim 2$  eV; at  $2.75 \pm 0.1$  for LSMO.125, at  $2.6 \pm 0.1$  eV for LCMO.3, at  $1.9 \pm 0.1$  eV, for PCMO.4 and at  $2.0 \pm 0.1$  for NSMO.5. This “2 eV” feature is reminiscent of the one observed in manganites in optical conductivity studies [3, 5]. Note that there is an apparent trend in this feature to move to lower energies with higher doping. Inami *et al.* reported a similar feature at  $2.5 \pm 0.25$  eV in  $\text{LaMnO}_3$  [6], which fits into this same trend. They ascribed this excitation to an orbital excitation. The data for PCMO.4 show that this feature is still present on warming through the orbital ordering transition ( $T_{OO} = 234$  K) and that therefore this feature cannot be associated with long-range orbital order. More generally, our data suggest that some contribution of the spectral weight about 2 eV is temperature independent - see in particular the NSMO.5 data. Thus, the temperature dependence of the low energy spectrum does not appear to be related to the

“2eV” feature, but rather moves to higher energies with higher doping (arrows in Fig. 2). We now discuss this temperature dependence in detail.

In order to characterize the low energy ( $< 6$  eV) spectra in a model-independent way, we have simply summed the intensity between 1.5 eV and 5 eV. This integrated intensity vs temperature is shown as closed circles in the right panels of Fig. 2. These panels illustrate the central result of this paper, namely that the integrated spectral weight between 1.5 and 5 eV follows the magnetization of the sample in a systematic way, and that this result is independent of the conductivity of the ground state.

Specifically, for LSMO.125, LCMO.3 and NSMO.5 the integrated intensity increases on cooling into a ferromagnetic metallic phase. Conversely, the intensity is seen to drop on entering an antiferromagnetic phase (PCMO.4 and NSMO.5). Finally, in LSMO.125 ( $T_{MI}=150$  K), there is a smooth increase in intensity as this sample is cooled through  $T_{MI}$  into the ferromagnetic insulating phase. Thus, we conclude that the change in the inelastic scattering reflects the magnetic order not the electrical conductivity. We note that the presence of the large quasi-elastic scattering dazzles the energy range below 1 eV where the closing of the gap associated with the onset of metallicity occurs.

These observations raise questions as to why does the inelastic scattering depend on the spin correlations and what is the relationship between the RIXS spectra and any calculable response function? In the following, we address these issues with density functional calculations within the LDA+ $U$  approximation.

We begin by calculating the electronic structure of the undoped  $\text{LaMnO}_3$  in a structure with the actual Jahn-Teller (JT) distortions of the octahedra (but without tilting), taking  $U = 8$  eV and  $J_H = 0.88$  eV (Fig. 3). We find a ground state with A-type antiferromagnetic order and an insulating gap. The gap results from a lifting of the degeneracy between the quarter-filled  $e_g$  states that accompanies the in-plane orbital ordering (and driven by the large on-site repulsion [10, 11]). These findings are consistent with the actual ground state of  $\text{LaMnO}_3$ . The upper panel of Fig. 3 shows that the only states relevant to the low-energy excitations are the  $e_g$  states of the majority spin at the Mn sites. The real space charge density of these states is illustrated in the lower panel, in which the Wannier functions of both the occupied ( $e_g^{\text{occ}}$ ) and the unoccupied ( $e_g^{\text{unocc}}$ ) states, either side of the Fermi level, are given for two neighboring sites [12, 13]. In addition to the staggered orbital ordering of the  $e_g^{\text{occ}}$  states, the unoccupied  $e_g^{\text{unocc}}$  states are spatially orthogonal to the  $e_g^{\text{occ}}$  states at the same site.

With these results in hand, the mechanism for the observed temperature dependence of the RIXS spectra can be understood in the following way: In the small- $q$  region, the low-energy features in the RIXS spectra are dominated by *inter-site*  $d-d$  transitions between Mn atoms (mediated via the hybridization with the O-2p states as evidenced by the Wannier functions in Fig. 3). Ignoring improbable spin-flip excitations, such inter-site transitions can only occur between

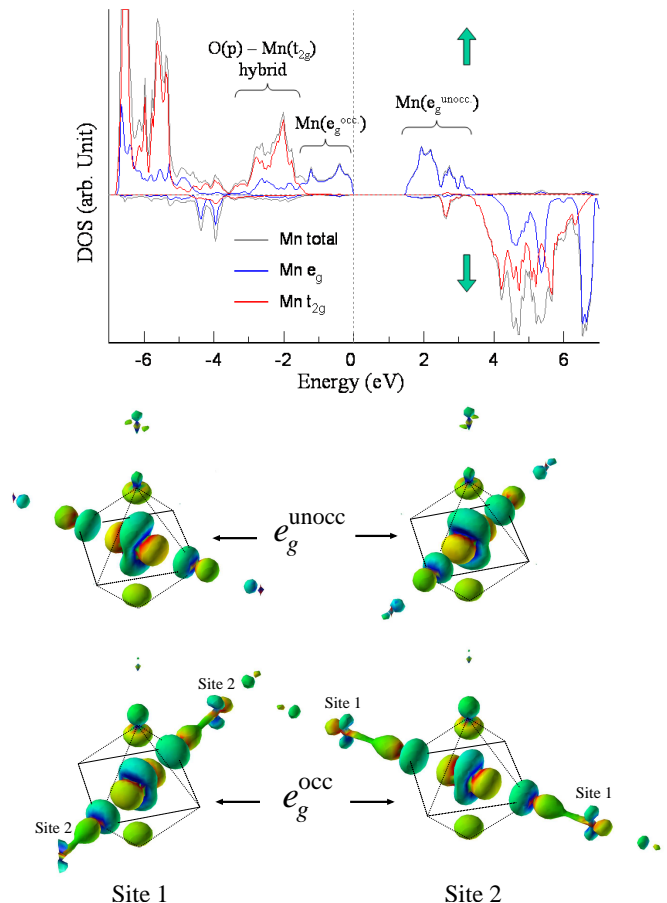


FIG. 3: (Upper panel) Density of states on Mn atoms near the Fermi level for  $\text{LaMnO}_3$  calculated by LDA+ $U$ . (Lower panel) Wannier functions from the LDA+ $U$  calculations for  $e_g^{\text{unocc}}$  and  $e_g^{\text{occ}}$ . The oxygen octahedra are depicted. Site 1 and site 2 are two first neighbor Mn on the a-b plane ( $Pbnm$  setting).

neighbors with the same spin alignment, since no states exist at low energy in the opposite spin channel. This is illustrated schematically in Fig. 4a. Thus the more pairs of ferromagnetically aligned neighbors in the system, the stronger the low-energy spectra will be, consistent with our experiments.

This simple picture was confirmed by calculations of the dielectric function,  $\varepsilon(q, \omega)$ , whose imaginary part reflects the spectrum of allowed transitions (Fig. 4b) [12, 14]. The calculation was performed twice with the JT-distorted, untilted, structure: Once for the A-type AF magnetic ordering, and once for a ferromagnetic ordering. The momentum transfer was taken to be similar to that of the experiments, after mapping back to the first Brillouin zone. We find that the ferromagnetic dielectric function is doubled relatively to the AF one (Fig. 4b), as is  $S(q, \omega)$  at low energies (not shown). This enhancement results from the additional charge transfer along the c-axis, via the apical O (Fig. 3), which is suppressed in the AF case. This additional contribution is of similar size to that arising from transitions within the a-b plane because, despite the ferromagnetic correlations of the four Mn nearest

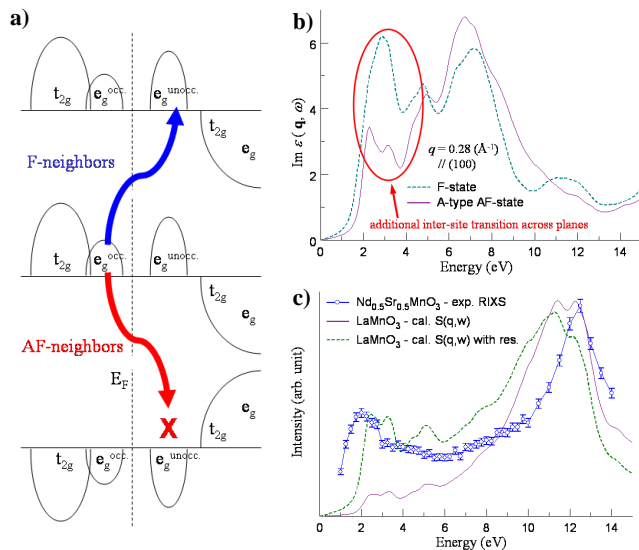


FIG. 4: a) Schematic for the possible hopping between neighboring sites. For ferromagnetic neighbors, low energy excitations are allowed. For antiferromagnetic neighbors, such excitations require an improbable spin-flip and are suppressed. b) Imaginary part of the dielectric function for two magnetic ground states of  $\text{LaMnO}_3$ . c) Comparison between the RIXS spectra for the AFI NSMO.5 and the calculated  $S(q, \omega)$  for AFI  $\text{LaMnO}_3$ , with and without the resonant factors (see text).

neighbors in-plane, only two contribute due to the directional nature of the ordered orbitals - as illustrated by the Wannier functions (Fig. 3). In the actual doped systems, this difference may be reduced for various reasons, including changes in orbital ordering, degree of hybridization, the bandwidth of the  $e_g$  states, and screening due to metallization. However, the qualitative trend is expected to persist and explains the present results.

Our first principles calculations also allow us to discuss the connection between the RIXS cross-section and a calculable response function. Several authors have argued that for  $K$ -edge resonant IXS, the cross-section is proportional to the IXS cross-section,  $S(q, \omega)$  (which is proportional to  $\text{Im}(\frac{-1}{\epsilon})$ , the loss function) multiplied by a term accounting for the resonance [15, 16, 17]. In Fig. 4c we show a comparison between the NSMO.5 data (low temperature AFI) and the calculated  $S(q, \omega)$  for  $\text{LaMnO}_3$  (low temperature AFI), weighted or not by the resonant factor. It is seen that the weighted  $S(q, \omega)$  closely resembles the data, clearly suggesting that there is a connection between the two, though this requires more work before a firm conclusion can be drawn.

Before concluding, we briefly comment on the high energy portion of the spectra. The 8 eV region has little temperature dependence except for  $\text{LSMO.125}$  which exhibits a clear drop on cooling through  $T_C = 190$  K with a continuous decrease through the orbital ordering transition at  $T_{OO} = 150$  K. In Fig. 4a, we see that the 8 eV region corresponds to transitions from the majority states to the minority states of an AF

neighbor. The decrease within a ferromagnetic phase is therefore consistent with our picture. As to the 12 eV feature, it was observed in  $\text{LaMnO}_3$  with RIXS [6] and was attributed to a transition involving Mn states. Conversely, no excitation is seen around 12 eV in the optical spectra of the manganites [3, 18]. As shown in Fig. 2, substituting the earth cations does not significantly change the position of this feature, implying that their electronic states are not involved. In fact, it appears clearly here as a feature in  $S(q, \omega)$  (Fig. 4c) and our calculations suggest that it is more of a collective response of the system as a whole, *i.e.* a plasmon, as  $|\epsilon|$  reaches a low minimum.

In summary, we have measured temperature dependence in the inelastic x-ray scattering spectra of several manganites up to 10 eV energy loss. In the lowest energy range, we find that the excitation spectrum does not depend on the presence or absence of orbital order, but does correlate with the magnetic order of the sample. We calculated the DOS for  $\text{LaMnO}_3$  as well as the Wannier functions for the  $e_g$  states and describe the magnetic order dependent feature as arising from inter-site  $3d$ - $3d$  excitations. This work points to the sensitivity of the RIXS technique to magnetic correlations in manganites in addition to the charge excitations.

We acknowledge fruitful discussions with P. Abbamonte, V. Oudovenko, J. Rehr, J. van den Brink and M. van Veenendaal. Use of the Advanced Photon Source was supported by the U.S. DOE, Office of Basic Energy Sciences, under Contract No. W-31-109-Eng-38. Brookhaven National Laboratory is supported under DOE Contract No. DE-AC02-98CH10886. Supports from the NSF MRSEC program, Grant No. DMR-0080008 and from the NSF Grant No. DMR-0093143 are also acknowledged.

- 
- [1] M. B. Salamon and M. Jaime, *Rev. Mod. Phys.* **73**, 583 (2001).
  - [2] E. Dagotto, T. Hotta, and A. Moreo, *Physics Report* **344**, 1 (2001).
  - [3] Y. Okimoto, T. Katsufuji, T. Ishikawa, T. Arima, and Y. Tokura, *Phys. Rev. B* **55**, 4206 (1997).
  - [4] J. H. Jung, K. H. Kim, D. J. Eom, T. W. Noh, E. J. Choi, J. Yu, Y. S. Kwon, and Y. Chung, *Phys. Rev. B* **55**, 15489 (1997).
  - [5] M. Quijada, J. Cerne, J. R. Simpson, H. D. Drew, K. H. Ahn, A. Millis, R. Shreekala, R. Ramesh, M. Rajeswari, and T. Venkatesan, *Phys. Rev. B* **58**, 16093 (1998).
  - [6] T. Inami, T. Fukuda, J. Mizuki, S. Ishihara, H. Kondo, H. Nakao, T. Matsumura, K. Hirota, Y. Murakami, S. Maekawa, et al., *Phys. Rev. B* **67**, 045108 (2003).
  - [7] C. C. Kao, W. A. L. Caliebe, J. B. Hastings, and J.-M. Gillet, *Phys. Rev. B* **54**, 16361 (1996).
  - [8] W. Schülke, *J. Phys. Cond. Matt.* **13**, 7557 (2001).
  - [9] J. W. Lynn, R. W. Erwin, J. A. Borchers, Q. Huang, A. Santoro, J.-L. Peng, and Z. Y. Li, *Phys. Rev. B* **76** (1996).
  - [10] V. I. Anisimov, I. S. Elfimov, M. A. Korotin, and K. Terakura, *Phys. Rev. B* **55**, 15494 (1997).
  - [11] D. Volja, W. Ku, T. Vogt, and J. Davenport, unpublished (2004).
  - [12] W. Ku, W. E. Pickett, R. T. Scalettar, and A. G. Eguiluz, *Phys. Rev. Lett.* **88**, 057001 (2002).

- [13] W. Ku, H. Rosner, W. E. Pickett, and R. T. Scalettar, Phys. Rev. Lett. **89**, 167204 (2002).
- [14] Wei Ku *et al.*, unpublished (2004).
- [15] P. M. Platzman and E. D. Isaacs, Phys. Rev. B **57**, 11107 (1998).
- [16] P. Abbamonte, C. A. Burns, E. D. Isaacs, P. M. Platzman, L. L. Miller, S. W. Cheong, and M. V. Klein, Phys. Rev. Lett. **83**, 860 (1999).
- [17] J. van den Brink and M. van Veenendaal, cond-mat/0311446 (2003).
- [18] T.-h. Arima and Y. Tokura, J. Phys. Soc. Jap. **64**, 2488 (1995).